Journal of Physical and Theoretical Chemistry
of Islamic Azad University of Iran, 19 (2) 25-39: Summer 2022
(J. Phys. Theor. Chem. IAU Iran)
ISSN 1735-2126

Response Surface Methodology for Removal of Butyl Paraben Dye Using Zeolitic Imidazolate-67 Modified by Fe_3O_4 Nanoparticles from Aqueous Solutions

Mohammad Pourmohammad[1], Arezoo Ghadi[1]*, Ali Aghababai Beni[2]

[1] Department of Chemical Engineering, Ayatollah Amoli Branch, Islamic Azad University, Amol, Iran
[2] Department of Chemical Engineering, Shahrekord Branch, Islamic Azad University, Shahrekord, Iran

Received January 2023; Accepted March 2023

ABSTRACT

The applicability of Zeolitic Imidazolate-67 Modified by Fe_3O_4 Nanoparticles, was studied for eliminating butyl paraben dye from aqueous solutions. Identical techniques including BET, IR, XRD, and SEM have been utilized to characterize this novel material. The impacts of variables including initial butyl paraben concentration (X_1), pH (X_2), adsorbent dosage (X_3), and sonication time (X_4) came under scrutiny using central composite design (CCD) under response surface methodology (RSM). Additionally, the impacts of the pH of the solution, the amount of nanoparticles, concentration of butyl paraben dye, and contact time were investigated. The experiments have been designed utilizing response surface methodology. In this current article the values of 10 mgL^{-1} , 0.03 g, 7.0, 4.0 min were considered as the ideal values for butyl paraben concentration, adsorbent mass, pH value and contact time respectively. The kinetics and isotherm studies proved the appropriateness of the second-order and Langmuir models for the kinetics and isotherm of the adsorption of butyl paraben on the adsorbent. The adsorbent was proved to be recyclable for more than once. Since almost 99.5% of butyl paraben was deleted with ideal adsorption capacities of 110 mgg^{-1} for butyl paraben in no time, therefore not only the short-time adsorption process was considered an advantage but also vantages in using Zeolitic Imidazolate-67 Modified by Fe_3O_4 Nanoparticles like being recyclable, safe, and cost-efficient made it a promising and powerful material for the aqueous solutions.

Keywords: Butyl Paraben; Adsorption; Zeolitic Imidazolate-67; Central Composite Design (CCD); Response Surface Methodology (RSM).

1. INTRODUCTION

Industrial wastewater as an undesirable by-product may be released to a sanitary sewer or surface water in the environment. Therefore this issue has been among the most serious environmental concerns to keep an eye on. It requires considerable time and effort to blanch their high color and organic concentrations [1]. Parabens are chemically esters of p-hydroxybenzoic acid and are a class of widely used

* Corresponding author: arezoo.ghadi@gmail.com

artificial preservatives and antimicrobial in many PCPs (personal care products) as well as pharmaceutical products [2], food, beverages and industrial products. The use of parabens in sunscreen creams, toothpastes, cosmetics, glues, fats and oils is inevitable and their use in a variety of consumer products is undeniable [3]. Also some scholars in their published studies have associated the high concentrations of parabens with male reproductive disorders. However, paraben has found its way to wastewater plants due to its large mentioned application. Some wastewater treatment technologies were successful in removing a considerable amount of parabens from wastewater [4]. Moreover, the presence of parabens in soil and sediment samples has been confirmed. Accordingly, the necessity of removing toxic dyes from industrial wastewater before discharging has turned into a global concern [5]. For removing dyes from aqueous media, different methods of coagulation, precipitation, adsorption, membrane filtration, electrochemical techniques, ozonation, and Sorption have been practiced [6-9]. Particularly, adsorption has drawn the attention of the worldwide researchers thanks to its simplicity in operation, high efficiency, and its inexpensive operation cost [10,11]. In improving removal efficiency, detecting novel adsorbent materials has always been the most prominent issue in adsorption [12]. Nanotechnology as an inviting area of research principally focuses on developing nanoparticles with varied sizes, chemical compositions, shapes, and possible application that can serve for the benefit of mankind [13]. The physical and chemical characteristics of the adsorbent are effective to a great extent on the efficacious applicability of an adsorption process. Amongst these characteristics, having great adsorption capacity and being renewable, available, and affordable are mentionable. Nowadays, a lot has been done by testing different potential adsorbents to find out whether they are successful in removing specific organics from water samples. From this perspective, numerous studies have been done on magnetic nanoparticles (MNPs) as unique adsorbents with high adsorption capacity, large surface area, and small diffusion resistance. They have been employed for separation of chemical species like environmental pollutants, metals, dyes, and gases [14-16].

The conventional adsorbents in terms of selectivity and capacity have been emerged as a fundamental problem. In recent years, metal-organic frameworks (MOFs) owing to their high surface area and porosity, a high capacity for adsorption, and desirable guest-host interactions, have been employed as a promising alternative in various applications such as drug delivery, adsorption processes [17]. Zeolitic Imidazolate Frameworks (ZIFs) represent a special class of Metal-Organic Frameworks (MOFs), formed by imidazole linkers and zinc or cobalt ions, resulting in micro porous crystalline structures with characteristics of both MOFs and zeolites [18,19]. ZIFs possess unique porous structures with open frameworks, adjustable cage pore structures, large surface areas, abundant functionalities, and enhanced thermal and chemical stabilities, which led them to a wide range of potential applications including adsorption, catalysis, separation, and sensing [20,21].

High adsorption capacity of the MOFs has been attributed to the electrostatic interactions, conjugated π-π interactions and hydrogen bonds. Since the MOFs show good thermal and chemical stability, they are utilized in a variety of applications, including gas adsorption, molecular separation, and electrochemistry. One of the most studied metal organic frameworks is the Zeolite

Imidazolate-67 (ZIF-67), which consists of Co^{2+} ions linked by 2-methylimidazolate to create a crystalline cubic structure with the parameters a = b = c = 16.9585 Å. ZIF-67 offers a three-dimensional (3D) structure with a high tendency to adsorb contaminants in the aqueous media. However, the application of ZIF-67 as an adsorbent still faces three vital problems including low specific surface area, poor structural stability, and difficult separation [22]. Porous magnetite nanoparticles (Fe_3O_4), as a result of their attractive potential applications as an interesting class of crystalline materials, have provided great agreement of consideration [23]. The size and shape-controlled synthesis of nano-scaled magnetite has been of considerable interest recently [22-24].

The synthesis of these unique adsorbents named Zeolitic Imidazolate-67 Modified by Fe_3O_4NPs was easily carried out and subsequently through the instrumentality of scanning electron microscopy (SEM), Fourier transform infrared spectroscopy (FTIR) and X-ray diffraction (XRD) analysis, they were characterized. Therefore, preparing ZIF-67 Modified by Fe_3O_4NPs as an alternative to exorbitant or noxious adsorbents for the elimination of (BP) dye from wastewater attracted our attention. In the process of (BP) dye deletion, shows structured (BP) dye in Fig. 1, In (BP) dye elimination process, with the help of CCD (central composite design) under RSM (response surface methodology), the scrutinizing and optimizing of the ensuing experimental conditions were performed: 1-pH of the solution, 2- contact time, 3-initial (BP) dye concentration, 4-adsorbent dosage and 5-the dye removal percentage. This fact that the adsorption of (BP) dye follows the pseudo-second-order rate equation was clearly proven. Furthermore, it was demonstrated that the Langmuir model could undoubtedly be used for the equilibrium data explanation. The pseudo-second-order model was in control of the kinetic of adsorption process which was confirmed through the analysis of kinetic models (both pseudo-first-order, pseudo-second-order diffusion models). The capability of Zeolitic Imidazolate-67 Modified by Fe_3O_4NPs in eliminating of (BP) dye from aqueous solutions was demonstrated by evidences.

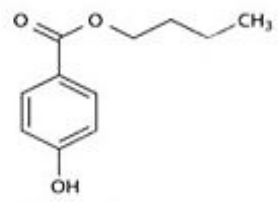

Fig. 1. The structures of butyl Paraben (BP) dye.

2. EXPERIMENTAL

2.1. Chemical and instruments

All the chemicals used are of the highest purity, and purchased from Merck (Darmstadt, Germany). Buthyl paraben (BP) dye (99%), Ammonium heptamolybdate (99%), and Iron nitrate (III) (98.0%). The standard and experimental solutions were obtained by diluting the stock solutions with deionized water. The applied instruments were as follow: Dyes concentrations were determined using Jasco UV–Vis spectrophotometer model V-530 (Jasco Company, Japan). IR spectra were registered on a (PerkinElmer company, Germany). SEM (Phillips, PW3710, Netherland), used to study the morphology of samples.

2.2. Synthesis of ZIF-67

According to the literature, ZIF-67 nano-cubes were synthesized using a simple approach in aqueous solution at RT ZIF-67 nano-cubes were prepared via a simple method in aqueous solution at RT according to the literature [25].

2.3. Synthesis of ZIF-67 Modified by Fe_3O_4NPs

ZIF-67 Modified by Fe_3O_4NPs was briefly fabricated by 0.86 g of $FeCl_2{\cdot}4H_2O$, 2.35 g $FeCl_3{\cdot}6H_2O$ (molar ratio of Fe^{2+}: Fe^{3+}=1:2) and 1.5 g ZIF-67 were dissolved in 40 ml of deoxygenated water with vigorous stirring at a speed of 500 rpm. 40 ml of NH_4OH (25%) was added slowly after the solution was heated to 60°C. First, 30 mg of ZIF-67 was dispersed in 30 mL of double distilled water in an ultrasonic bath. Afterwards, $KMnO_4$ (in excess, a full spatula) was added and stirred for 6h. After that, the white precipitate was then washed multiple times with water and ethanol and dried overnight at 50°C. Then the white precipitate was washed with water and ethanol several times, and dried at 50°C overnight. The sediment suspension was stirred for 3 hours. Stirring was stopped and the suspension was placed in the laboratory for 2 hours. The ZIF-67 Modified by Fe_3O_4NPs produced suspensions were prepared from a leaf medlar with an equal weight ratio and after analysis, BET, IR, XRD and SEM were used as adsorbent [26].

2.4. Adsorption experiments

Based on the experimental conditions in the CCD, the adjustment of the pH of different solutions with different concentration of (BP) dye was carried out utilizing concentrated HCl, and/or NaOH. Through using an Erlenmeyer flask (50 mL), they were mixed completely with exact amounts of adsorbent [2]. The trials were done at ambient temperature during predetermined sonication time in an ultrasonic. In the twilight of the adsorption process, the centrifugation of the sample solution was done promptly and the analysis of the supernatant containing residual was performed using UV-Vis spectroscopy. The equilibrium concentrations and removal efficiency (%) of the (BP) dye were calculated according to equations (1) and (2), respectively. All experiments the final results were presented as mean values.

$$R\% = \frac{C_0 - C_e}{C_0} \times 100 \quad (1)$$

$$q_i = \frac{V(C_0 - C_e)}{M} \times 100 \quad (2)$$

C_0 (mg/L) in the formula refers to the initial (BP) dye concentration, and C_e (mg/L) represents the equilibrium (BP) dye concentration in an aqueous solution. V (L) shows the solution volume, and W (g) signifies the mass adsorbent [27,28].

2.5. Ultrasound Assisted method

Through the instrumentality of ultrasound assisted method, the elimination of (BP) dye in an adsorption combined with ZIF-67 Modified by Fe_3O_4 NPs was scrutinized. In a batch mode, the sonochemical adsorption trial was performed in the following way: the Erlenmeyer flask was loaded with exact quantities of (BP) dye solution (50 mL) at specified concentration 10.0 mg L^{-1}, and pH of 7.0 with a known quantity of adsorbent (0.03 g) while the desired sonication time (4 min) was maintained at the 25°C. It is worth mentioning that all utilized solutions were prepared per day with desired concentrations by diluting the stock solution with DW (double distilled water). The adsorption trials were executed in a batch mode and the solution was ultrasonicated at conditions devised under RSM. After performing the centrifugation for 4 min, the adsorbent ZIF-67 Modified by Fe_3O_4 NPs were separated. The analysis of the dilute phase was done for determining (BP) dye concentration with the help of UV–Vis spectrophotometer at wavelength of 370 nm [6, 28].

2.6. Central composite design (CCD)

Central composite design (CCD) method is applied not only to decrease the number of

trials and expenses but also to analyze the impact of parameters via designing experimental runs [2, 28]. In this article, design expert software (version 7.0) was utilized for the analysis of the CCD outcomes. These parameters were considered: initial (BP) dye concentrations (X_1), pH (X_2), adsorbent mass (X_3) and contact time (X_4). As shown in (Table. 1, and 2), the number of trials was 31 at 5 levels: (-α (-2), low (-1), center (0), high (+1) and +α (+2)). To examine the reliability and validity of the developed model, ANOVA (analysis of variance) was employed. The lack of fit, regression coefficient (R^2) and the Fisher test value (F-value) were determined. With the help of second-order polynomial response equation, the mathematical relationship between the five independent parameters was obtained constantly [6, 29].

2.7. Desirability function

Desirability function or DF designs a function for each specific response that provokes the final output of the general function (D) and the highest value of this output guarantees the achievement of optimum value. The governing principle and application of desirability function for the finest prognostication of real behavior of sorption system was mentioned before [28,29]. In the desirability profiles, the predicted levels of variables that can create the most favorable responses are recorded.

3. RESULTS AND DISCUSSION

3.1. Characterization of adsorbent

3.1.1. BET; analysis of ZIF-67 Modified by Fe_3O_4 NPs.

BET analysis was used to study the physicochemical properties of ZIF-67 Modified by Fe_3O_4 NPs. Fig. 2a shows the related N_2 adsorption-desorption isotherm, which clearly exhibits a type-IV isotherm with a noticeable hysteresis loop in the P/P_0 region of 0.3-0.95. The corresponding N_2 adsorption-desorption isotherm is shown in Figure 5a, where a type-IV isotherm is clearly visible with a distinct hysteresis loop in the P/P_0 range of 0.3-0.95. The specific surface area of the ZIF-67 Modified by Fe_3O_4 NPs was found to be 203.78 $m^2.g^{-1}$. The corresponding BJH pore distribution curve (Fig. 2b) was used to evaluate the pore structure of ZIF-67 Modified by Fe_3O_4 NPs. As can be seen, two distinct types of pores were observed: microspores (2 nm) and mesospores (2-50 nm), with an average pore width of 4.179 nm [30].

3.1.2. FT-IR, XRD, and SEM analysis

FT-IR, XRD, and SEM measurements were used to characterize the adsorbent structural characterization of the adsorbent were carried out by FT-IR and SEM analyses. Fig. 2a displays the FTIR spectrum of ZIF-67 [30]. As can be seen, all FT-IR spectra exhibit broadband covering the 3300 to 3500 cm^{-1} range, with an absorption band observed at 2928 cm^{-1} for stretching vibrations of OH groups and C-H bonds, respectively Two other

Table 1. Experimental factors, levels and matrix of CCD

Factors	levels			Star pointα = 2.0	
	Low (-1)	Central (0)	High(+1)	-α	+α
(X_1) BP Concentration (mg L^{-1})	10	15	20	5	25
(X_2) pH	4.0	6.0	8.0	2.0	10.0
(X_3) Adsorbent mass (g)	0.0150	0.0225	0.0350	0.005	0.045
(X_4) Sonication time (min)	3.0	4.0	6.0	2.0	8.0

Table 2. The design and the response

Run	X_1	X_2	X_3	X_4	R% (BP) dye
1	20	6	0/025	4	95.0
2	25	8	0/015	3	67.0
3	10	4	0/015	6	96.0
4	20	6	0/025	4	93.0
5	25	4	0/015	3	72.0
6	10	8	0/035	3	100.0
7	20	4	0/025	4	96.1
8	20	6	0/025	8	95.2
9	10	4	0/035	3	80.1
10	10	4	0/015	5	90.5
11	20	6	0/025	4	95.0
12	25	8	0/015	6	71.0
13	20	8	0/035	6	83.2
14	10	8	0/015	3	97.5
15	20	6	0/025	4	94.5
16	25	4	0/035	6	92.6
17	20	6	0/025	4	94.7
18	10	4	0/015	3	95.0
19	10	8	0/015	6	99.0
20	10	4	0/035	6	97.0
21	10	8	0/035	6	100.0
22	40	6	0/025	4	59.6
23	30	8	0/035	3	65.0
24	20	6	0/025	4	93.3
25	20	6	0/025	4	95.0
26	10	6	0/005	4	92.0
27	20	6	0/025	2	50.0
28	20	10	0/025	4	86.0
29	10	4	0/035	3	97.0
30	10	7	0/045	4	100.0

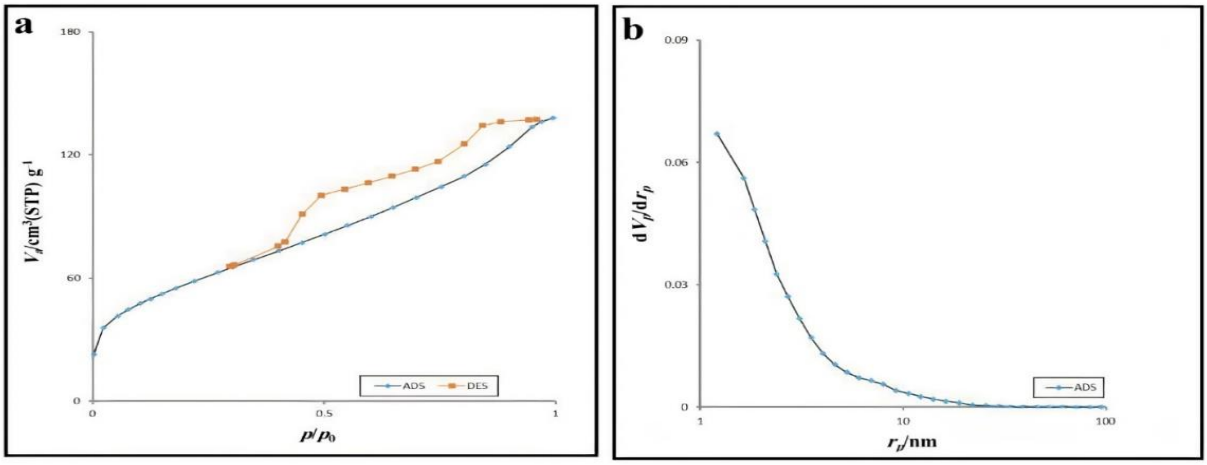

Fig. 2. (a) The N2 adsorption-desorption isotherm of ZIF-67 Modified by Fe_3O_4 NPs, and (b) its corresponding BJH pore distribution curve.

absorption bands were observed at 1000 and 1153 cm^{-1} rings for the C-O and bonds (C-O-C bridge), respectively Two peaks were also observed at 1621 cm^{-1} Fig. 3a and 1625 cm^{-1} for H-O-H bending vibrations of adsorbed water [30]. An extremely sharp band was seen at 572 cm^{-1} for FT-IR spectra of both the ZIF-67 (a) and ZIF-67-Fe_3O_4NPs (b), corresponding to stretching vibrations of the Fe-O bond, suggesting a reaction between ZIF-67 and magnetic Fe_3O_4 nanoparticles [30]. The C=C vibrations of the ZIF-67 structure were appeared at 1504 cm^{-1}. Figure 2c, on the other hand, represents the FTIR spectrum of the ZIF-67-Fe_3O_4NPs. One can note that the corresponding peaks of the anticipated functional groups are present in the final product, without considerable changes in their position and intensity [31,32]. The ZIF-67-Fe_3O_4NPs (b) XRD patterns were compared to the standard Fe_3O_4 (a) XRD pattern. The two samples showed the characteristic Fe_3O_4 peaks. An intense characteristic diffraction peak can be seen for the standard patterns of Fe_3O_4 (JCPDS card #00-001-111) at 2θ = 74.73º, 63.06º, 57.23º, 53.73º, 43.34º, 35.75º, and 30.38º, respectively, corresponding to (533), (440), (511), (422), (400), (311), and (220) planes. Furthermore, a diffraction peak at 2θ = 23.04 was observed in the ZIF-67-Fe_3O_4NPs (b) magnetic nanoparticles, corresponding to the dextrin coating of Fe_3O_4 nanoparticles (Fig. 3b) [31,32]. Morphological study of the ZIF-67-Fe_3O_4NPs was carried out by SEM. Surface morphology of the ZIF-67-Fe_3O_4NPs is shown in (Fig. 4). Clearly, the ZIF-67-Fe_3O_4NPs is formed of many ultrafine nanoparticles in the range of 36-55 nm [31, 32].

3. 2. Modeling the process and statistical analysis

The variance analysis of all the linear, quadratic and interaction impacts of the three planning factors in relation to R% of (BP) dye is represented in (Table 2). As specified by the F-value and p-value (<0.05), the model was extremely successful in elimination of dyes in the polynomial equation with 95% confidence interval [28,32]. By considering the value of the determination coefficient for deleting dyes, it has been noticed that the

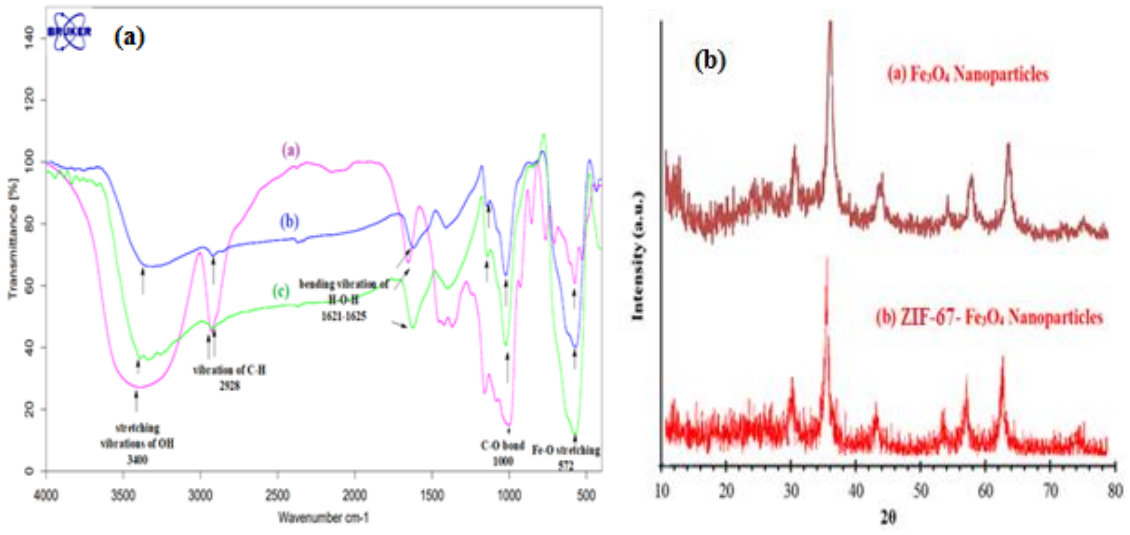

Fig. 3. (a) FTIR spectra of the prepared Fe_3O_4NPs, ZIF-67, ZIF-67-Fe_3O_4NPs. (b) Comparison of the XRD pattern of Fe_3O_4 NPs, and ZIF-67-Fe_3O_4NPs.

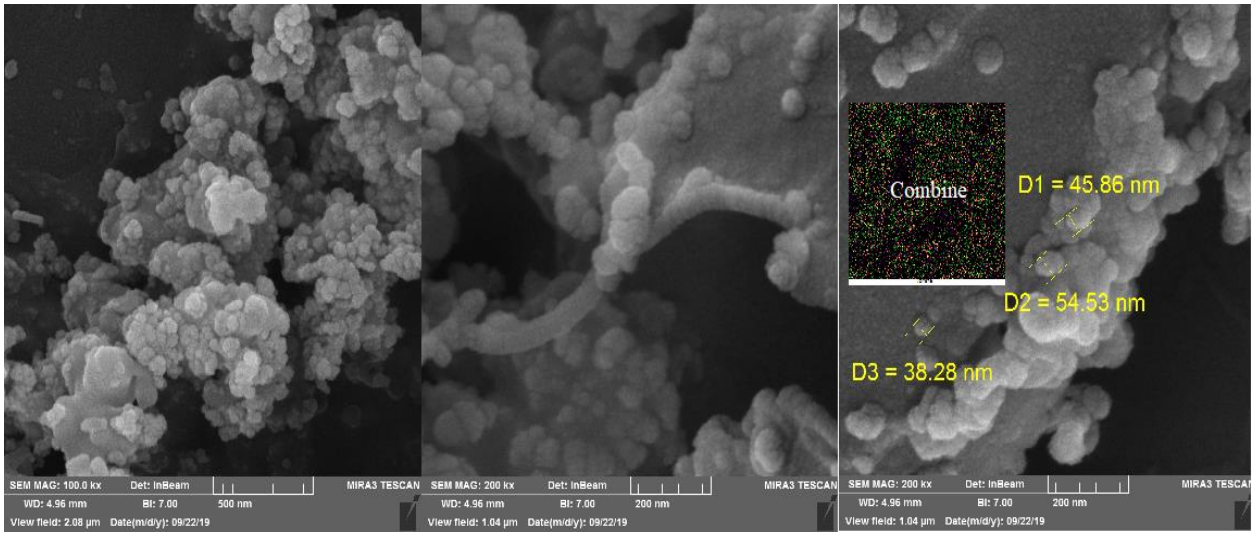

Fig. 4. The (SEM) image of the ZIF-67-Fe_3O_4NPs.

Table 3. Analysis of Variance for full quadratic model

Source of variation	Df	(BP) dye			
		Sum of square	Mean square	F-value	P-value
Model	14	4313.6	312.10	749..36	< 0.0001
X_1	1	1716.6	1716.6	4228.2	< 0.0002
X_2	1	283.21	283.21	649.13	< 0.0001
X_3	1	141.12	141.12	336.8	< 0.0000
X_4	1	426.15	426.15	1108.1	< 0.0001
X_1X_2	1	372.1	372.1	930.1	< 0.0002
X_1X_3	1	30.95	30.95	74.66	< 0.0000
X_1X_4	1	210.9	210.9	478.1	< 0.0001
X_2X_3	1	13.22	13.22	30.86	< 0.0000
X_2X_4	1	0.458	0.458	1.1926	0.28217
X_3X_4	1	3.112	3.112	7.501	0.0151
X_3X_5	1	225.9	225.9	547.12	< 0.0001
X_1^2	1	34.11	34.11	8201	< 0.0001
X_2^2	1	4.361	4.361	10.54	0.00512
X_3^2	1	154.37	154.37	372.63	< 0.0002
X_4^2	15	6.362	0.4311	752.16	< 0.0001
Residual	9	5.2252	0.56732		
Lack of Fit	6	1.0345	0.1791	3.3912	0.079496
Pure Error	29	4261.6			
Cor Total					

response surface quadratic model was a befitting model for predicting the function of dye adsorption on ZIF-67-Fe_3O_4NPs. The plots of experimental deletion % when juxtaposed against those computed from equations revealed a satisfactory fit. Eqs. (3). Represents the codified values for the quadratic equations after ruling out the insignificant terms.

$R\%(BP)\ dye = 93/084 - 10/093X_1 - 3/340X_2 + +2/4167X_3 + 4/2700X_4 - 4/9075X_1X_2 - 1/3925X_1X_3 + 3/5525X_1X_4 + 0/89500X_2X_3 - 0/17500X_2X_4 -$

$0/44000X_3X_4 - 3/7119X_1^2 - 1/1059X_2^2 + 0/39410X_3^2 - 2/3559X_4^2$ (3)

Where Y shows the predicted response (R% of dye), and the coded value of X_1 stands for the initial (BP) dye concentrations, X_2 for pH, X_3 and X_4 for the adsorbent mass and ultrasound time respectively. The significance of X1, X_2, X_4, X_5, X_1X_3, X_1X_4 and all quadratic impacts for R% of (BP) dye was verified.

3. 3. Response surface plots

Response surface methodology (RSM) was utilized to ameliorate the optimization and estimation of all significance interaction of variables and the relative significance on adsorption processes. Fig. 5, exhibits the three dimensional surface response plots of this interaction. The plots were prepared for a specified pair of factual factors at optimal and fixed values of other variables [24,33]. The interaction of variables is confirmed by looking at the curves in these plots. The interaction of adsorbent mass with initial concentration of Butyl Paraben dyes is represented in Fig. 5a. Increase in the adsorbent dosage led to a boost in the removal percentage on the grounds of availability of more active adsorption sites, high specific surface area, and small particle size. In Fig. 5b, the relevant interaction impact of sonication time on removal percentage is demonstrated. An increase was observed in the adsorption efficiency when time was increased under combined ultrasound/adsorbent process. In light of this figure, it is completely evident that at sonication time of 4 min, the highest dye adsorption was achieved. The optimization of the quadratic model equations was performed after verifying the relationship between the dependent and independent variables. The use of the desirability function was to assess how well a combination of levels of process parameters meets the goals and can produce the most satisfying responses on dye adsorption within the constraints (Table 4). To corroborate the optimum point for each parameter, additional experiments at the obtained optimal conditions were carried out in three replicates. Fig. 5, clearly represents the level of each process parameters, optimal response values and experimental outcomes. To achieve the maximum dye deletion of 100%, the optimum conditions were as follows: pH of 7.0, ultrasound time of 4 min, adsorbent mass of (0.03g) and initial dye concentration equal to (10 mgL^{-1}) for BP. Additionally, to examine the optimum conditions experimentally, eleven experiments under the same conditions at 25^0C was conducted. Based on the great conformity between the experimental and prediction data, it was confirmed that the central composite design could be utilized successfully for the evaluation and optimization of the influences of the adsorption independent variables on the removal efficiency of (BP) dye from aqueous media with the help of ZIF-67 Modified by Fe_3O_4 NPs [34,35].

Restricted to monolayer coverage and the surface was rather uniform with regard to the interaction of functional groups with (BP) dye molecule. The highest adsorption capacity for (BP) dye on the ZIF-67 Modified by Fe_3O_4 NPs was estimated to be 110 mgg^{-1}.

As can be seen, the max (BP) dye adsorption was attainable in short sonication time, which is a good indication of the big contribution of ultrasound power in mass transfer that result in the (BP) dye greater efficiency for the adsorption.

3. 4. Optimization of CCD by DF for Extraction Procedure

The profile for desirable option with predicted values in the STATISTICA 10.0 software was used for the optimization of the process (Fig. 6). The desirability in the

range of 0.0 (undesirable) to 1.0 (very desirable) was used to obtain a global function (*D*) that is the base of optimization. The CCD design matrix results were obtained as maximum (100 %) for (BP) dye, respectively. According to these values, DF settings for either of dependent variables of removal percentages were depicted on the right hand side of (Fig. 6).

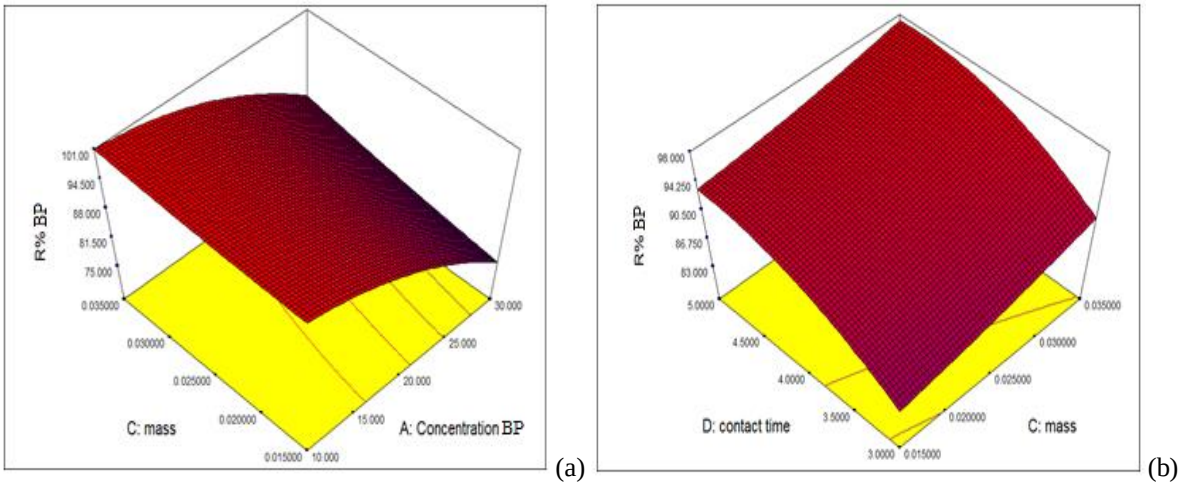

Fig. 5. 3-D surface plots for interactive impact of (a) adsorbent mass and initial (BP) dye concentration, (b) contact time and adsorbent mass.

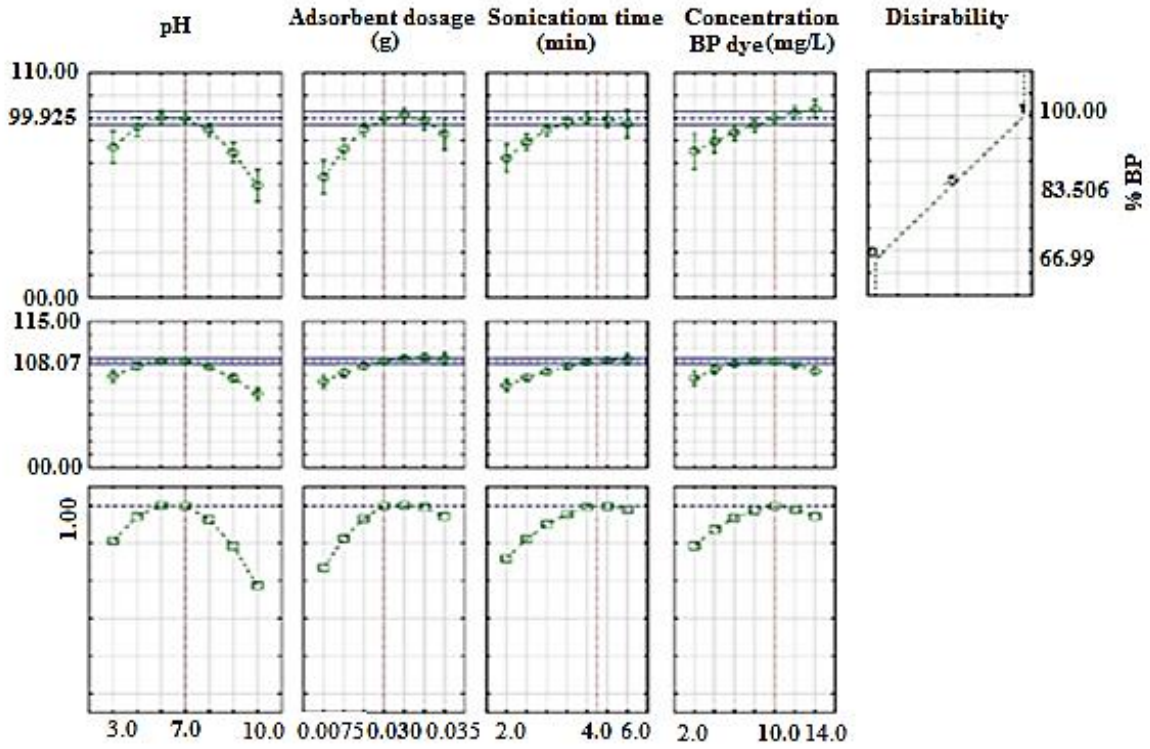

Figure. 6. Profiles for predicated values and desirability function for removal percentage of (BP) dye line indicates current values after optimization.

3.5. Adsorption equilibrium study

The experimental adsorption equilibrium data was evaluated for studying the mechanism of butyl paraben (BP) dye adsorption onto ZIF-67 Modified by Fe_3O_4 NPs using different models such as Langmuir, Freundlich and Temkin isotherms [36,37]. In their conventional linear form. Subsequently, their corresponding constants were evaluated from the slopes and intercepts of respective lines (Table. 4). These models were applied at optimal dosages of adsorbent while other variables were kept at optimal condition (Table. 4). Fitting the experimental data to these isotherm models and considering the higher values of correlation coefficients (R^2 = 0.991) for (BP) dye, it was concluded that the Langmuir isotherm is the best model to explain the (BP) dye adsorption onto ZIF-67 Modified by Fe_3O_4 NPs, which quantitatively describes the formation of a monolayer of adsorbate on the outer surface of the ZIF-67 Modified by Fe_3O_4 NPs. It also shows the equilibrium distribution of (BP) dye between the solid and liquid phase [38, 39].

3. 6. Kinetic study

In Table. 5, the values of the kinetic parameters of pseudo-first-order and second-order [38-40] models as well as qe,cal, qe,exp. and R^2 are represented. As evident, the estimation of the correlation coefficient in the pseudo-second-order equation for the adsorption of (BP) dye onto ZIF-67 Modified by Fe_3O_4 NPs was 0.999. It is worthy of note that the estimated values of qe, cal were in great conformity with the experimental data. Therefore it can be assumed that pseudo second-order rate process can appropriately describe the adsorption of (BP) dye onto ZIF-67 Modified by Fe_3O_4 NPs. The fitness of film diffusion model is indicated by the close to unity value of R^2. However, taking into account the fact that the straight lines did not pass through the origin indicate that resistance or film diffusion is not probably the sole rate-limiting step. The calculation of the Elovich constants is possible from the plots of qt versus lnt [40,41]. On the other hand, the inaptness of this model for the adsorption of (BP) dye onto ZIF-67 Modified by Fe_3O_4 NPs adsorbents is apparent from the low values of correlation coefficient (R^2) (Table. 5).

Table 4. Different isotherm constants and their correlation coefficients calculated for the adsorption of (BP) dye onto ZIF-67 Modified by Fe_3O_4 NPs

Isotherm	Equation	parameters	Value of parameters For (BP) dye
Langmuir	$q_e=q_m bC_e/(1+bC_e)$	Q_m (mg g^{-1})	110.0
		K_a (L mg^{-1})	0.460
		R^2	0.998
Freundlich	$\ln q_e = \ln K_F + (1/n) \ln C_e$	1/n	0.54
		K_F (L mg^{-1})	4.21
		R^2	0.953
Tempkin	$q_e = B_1 \ln K_T + B_1 \ln C_e$	B_1	15.6
		K_T (L mg^{-1})	6.71
		R^2	0.912
Dubinin-Radushkevich (DR)	$\ln q_e = \ln Q_s - B\varepsilon^2$	Q_s (mg g^{-1})	38.06
		$B\times 10^{-7}$	-1
		E (kj mol^{-1})	2281
		R^2	0.9312

3.7. Recycling of the adsorbent

The ability to recover, and reusing of the adsorbent was tested in several steps of adsorption, and desorption. The result is shown in (Fig. 7). As shown in Figure, 98% of (BP) dye was desorbed from the adsorbent after the first cycle, and after 6 cycles, there were slight changes in (BP) dye desorption. So, it was concluded that the desired removal of 98% could be achieved after 6 cycles [28, 41].

3. 8. Comparison of various adsorbent

A comparison of the maximum adsorption capacities of different adsorbents for the removal of Paraben dyes was also reported in (Table. 6). The outcomes of the table clearly show that the sorption capacity of utilized sorbent in the current study is significantly high. In general, morphology, particle size and distribution and surface structure of this sorbent were effective in its successful outcomes.

Table 5. Kinetic parameters for the adsorption of (BP) dye onto ZIF-67 Modified by Fe_3O_4 NPs

Model	Parameters	Value of parameters for (BP) dye
Pseudo-first-order kinetic $\log(q_e - q_t) = \log(q_e) - (\frac{k_1}{2.303})t$	k_1 (min^{-1}) qe (mgg^{-1}) R^2	0.996 17.12 0.9136
Pseudo-second-order kinetic $t_{/q_t} = \frac{1}{k_2 q_e 2} + \left(\frac{1}{q_e}\right)t$	k_2 (min^{-1}) q_e ($mg\ g^{-1}$) R^2	0.146 55.97 0.999
Intraparticle diffusion $q_t = k_{intra}(t)^{1/2} + C$	K_d ($mgg^{-1}\ min^{-1/2}$) C (mgg^{-1}) R^2	8.15 32.98 0.9774
Elovich $q_t = \frac{1}{\beta}\ln(\alpha\beta) + \frac{1}{\beta}\ln(t)$	β ($g\ mg^{-1}$) α ($mg\ g^{-1}\ min^{-1}$) R^2	0.917 17.94 0.9636

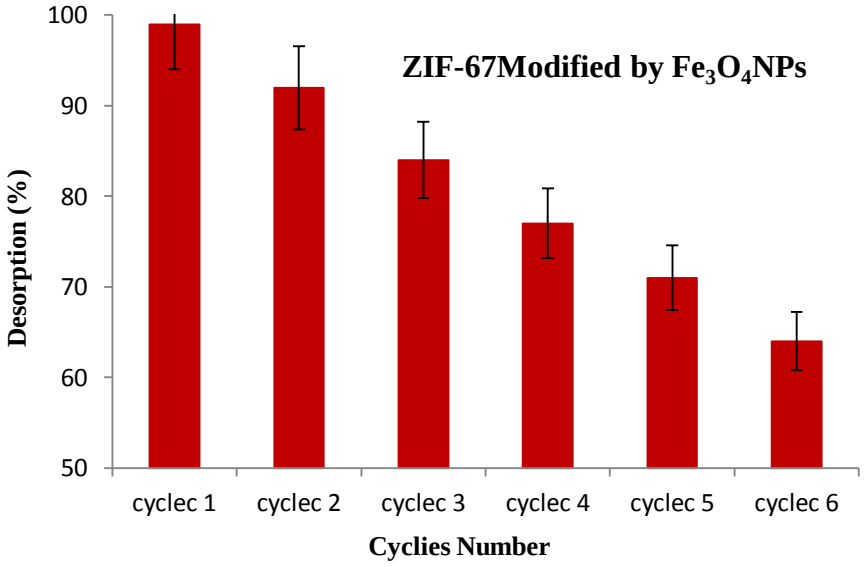

Figure. 7. Desorption of (BP) dye from ZIF-67 Modified by Fe_3O_4 NPs. [C_0= 10.0 mgL^{-1}, pH = 7.0, dosage sorbent = 0.03 g, time = 4.0 min, T=25^0C].

Table 6. Comparison of results for this work with other reported

Dye	Adsorbent	Dosage sorbent	pH	Time	Adsorption capacity	References
Methyl paraben (MP) dye	Zn (OH)2-NPs-AC	0.03 g	7.0	4 min	100.0 mgg^{-1}	[2]
Benzyl Paraben (BP) dye	Mn-doped PbS (PbS:Mn) NPs	0.1 g	2.0	15 min	145.0 mgg^{-1}	[3]
Butyl Paraben (BP) dye	ALLC AgNPs	0.025 g	5.0	5 min	100.0 mgg^{-1}	[6]
Propyl Paraben (PP) dye	TiO_2 NPs-AC	0.025 g	6.0	5 min	120 mgg^{-1}	[34]
Butyl Paraben (BP) dye	ZIF-67 Modified by Fe_3O_4NPs	0.03 g	7.0	4 min	110.4 mgg^{-1}	This work

4. CONCLUSION

A thorough investigation was performed on the effectiveness of synthesized ZIF-67 Modified by Fe_3O_4 Nanoparticles as an adsorbent for the deletion of (BP) dye from aqueous solutions. Response surface methodology was exercised to design the experiments and quadratic model was utilized for the prediction of the variables. With the help of central composite design (CCD) of RSM, the impacts of process variables including dye concentration, pH, adsorbent mass and contact time on adsorption of (BP) dye came under scrutiny. Under the conditions of pH of 7.0, (BP) dye concentration equal to 10 mgL^{-1}, adsorbent mass of 0.03 g, and sonication time of 4.0 min, the adsorption of (BP) dye onto ZIF-67 Modified by Fe_3O_4 Nanoparticles was almost 99.8%. The experimental removal efficiency of ZIF-67 Modified by Fe_3O_4 Nanoparticles got to (R^2= 0.999) for butyl paraben dye at optimal adsorption conditions. The excellent contribution of ZIF-67 Modified by Fe_3O_4 Nanoparticles in deleting (BP) dye was confirmed when the lowest errors were obtained in no time. Equilibrium adsorption revealed that the system followed the Langmuir model. The highest adsorption capacity value of (BP) dye with ZIF-67 Modified by Fe_3O_4 Nanoparticles was observed to be 110 mgg^{-1}. The kinetics studies brought to light that (BP) dye deletion followed pseudo second-order rate equation. Furthermore, desorption studies corroborated the possibility of recycling the adsorbent. With reference to the results of the linear regression-based analysis, it was reported that a satisfactory adsorbing performance onto ZIF-67 Modified by Fe_3O_4 Nanoparticles was predictable from the empirical models with significant determination coefficients of R^2= 0.998. In addition, the fact that the recommended equations could conveniently be utilized for the adsorption of (BP) dye from aqueous solutions was guaranteed by the statistical outcomes. Further considerations on the applicability of this adsorbent for the deletion of other materials have been highly recommended. ZIF-67 Modified by Fe_3O_4 Nanoparticles when juxtaposed against other adsorbents showed better performance in deleting (BP) dye from aqueous medium.

ACKNOWLEDGEMENT

The authors would like to acknowledge and thank the partial support of the Islamic Azad University, Branch of Ayatollah Amoli, Iran in this work.

REFERENCES

[1] D. Gryglik, M. Lach, J.S. Miller, Photochem. Photobiol. Sci. 8 (2009) 549-555.
[2] A. A. Ghazali, J. Phys. Theore. Chem. 18(1) (2021) 49-62.

[3] E. Mousavi, A. Geramizadegan, J. Phys. Theore. Chem. 17(3,4) (2021) 123-143.
[4] N. Karachi, S. Motahari, S. Nazarian, Desal. Water Treat. 228 (2021) 389-402.
[5] F. Maghami, M. Abrishamkar, B. Mombeni Goodajdar, M. Hossieni, Desal. Water Treat. 223 (2021) 388-392.
[6] F. Maghami, M. Abrishamkar, B. Mombini Godajdar, M. Hossieni, J. Appl. Chem. Res. 16(4) (2022) 45-64.
[7] M. Zarei, A. Niaei, D. Salari, A. Khataee, J. Hazard. Mater. 173 (2010) 544-551.
[8] S. Bagheri, H. Aghaei, M. Ghaedi, A. Asfaram, M. Monajemi, A.A. Bazrafshan, Ultrason. Sonochem. 41 (2018) 279-287.
[9] A. Omani Ziarati, Gh. Vatankhah, J. Phys. Theore. Chem. 18(2) (2021) 55-74.
[10] F. N. Azad, M. Ghaedi, K. Dashtian, S. Hajati, V. Pezeshkpour, Ultrason. Sonochem. 31 (2016) 383-393.
[11] N. N. Abd Malek, A.H. Jawad, A. S. Abdulhameed, K. Ismail, B.H. Hameed, Int. J. Biolog. Macromol.146 (2020) 530-539.
[12] A. Reghioua, D. Barkat, A. H. Jawad, A. S. Abdulhameed, A. A. Al-Kahtani, A. A. Al-Othman, J. Environ. Chem. Eng. 9 (2021) 105166.
[13] H. Pooladi, R. Foroutan, H. Esmaeili, Environ. Monitor. Assessment. 193(5) (2021) 1-19.
[14] S. Hajati, M. Ghaedi, H. Mazaheri, Desal. Water Treat. 57 (2016) 3179-3193.
[15] A. R. Parvizi, S. Bagheri, N. Karachi, Orient. J. Chem. 32 (2017) 549-565.
[16] S. Mosleh, M. Rahimi, M. Ghaedi, K. Dashtian, Ultrason. Sonochem. 32 (2016) 387-397.
[17] F. Yu, X. Bai, M. Liang, J. Ma, Chem. Eng. J. 405 (2021) 126960.
[18] L. Chen, X. Zhang, X. Cheng, Z. Xie, Q. Kuang, L. Zheng, Adv, Nanoscale. 2 (2020) 2628.
[19] A. Hassanpour, M. Zamanfar, S. Ebrahimiasl, A. Ebadi, P. Liu, Arab. J. Sci. Eng. 47 (2022) 477-484.
[20] M. Qiu, C. He, J. Hazard. Mater. 367 (2019) 339-347.
[21] P. Arabkhani, H. Javadian, A. Asfaram, M. Ateia, Chemosphere. 271 (2021) 129610.
[22] R. Foroutan, S. J. Peighambardoust, S. Hemmati, Int. J. Biolog. Macromol. 189 (2021) 432-442.
[23] F. Marahel, B. Mombeni Goodajdar, N. Basri, L. Niknam, A.A. Ghazali, Iran. J. Chem. Chem. Eng. 42(1) (2023) 1-22. doi: 10.30492/IJCCE.2021.527025.4636.
[24] Sh. Einolghozati, E. Pournamdari, N. Choobkar, F. Marahel, Desal. Water Treat. 278 (2022) 195-208.
[25] Y. Lü, W. Zhan, Y. He, Y. Wang, X. Kong, Q. Kuang, Z. Xie, L. Zheng, ACS. Appl. Mater. Interfaces, 6(6) (2014) 4186-4195.
[26] M. Shahbakhsh, M. Noroozifar, Biosens. Bioelectron. 102 (2018) 439-447.
[27] M. Arabi, M. Ghaedi, A. Ostovan, ACS Sustain. Chem. Eng. 5 (2017) 3775-3785.
[28] F. Marahel, B. Mombeni Goodajdar, L. Niknam, M. Faridnia, E. Pournamdari, S. Mohammad Doost, Int. J. Environ. Anal. Chem. 101(5) (2021) 1-22. https://doi.org/10.1080/03067319.2021.1901895.
[29] M. Kiani, S. Bagheri, N. Karachi, E. Alipanahpour Dil, Desal. Water Treat. 152 (2019) 366-378.
[30] A. Khan, M. Ali, A. Ilyas, P. Naik, I. F. Vankelecom, M.A. Gilani, M. R.

Bilad, Z. Sajjad, A. L. Khan, Sep. Purif. Technol. 206 (2018) 50-64.
[31] Y. Li, Z. Jin, T. Zhao, Chem. Eng. J. 382 (2020) 123051.
[32] A. R. Bagheri, M. Ghaedi, S. Hajati, M. Ghaedi, A. Goudarzi, A. Asfaram, RSC Adv. 5 (2015) 59335-59343.
[33] S. Bagheri, H. Aghaei, M. Ghaedi, M. Monajjemi, K. Zare, Eurasian J. Anal. Chem. 13(3) (2018) 1-10.
[34] M. Pargari, F. Marahel, B. Mombini Goodajdar, Desal. Water Treat. 212 (2021) 164-172.
[35] Sh. Ghanavati Nasab, A. Semnani, A. Teimouri, M. Javaheran Yazd, T. Momeni Isfahani, S. Habibollahi, Int. J. Biology. Macromol. 124 (2019) 429-456.
[36] S. Hajati, M. Ghaedi, B. Barazesh, F. Karimi, R. Sahraei, A. Daneshfar, A. Asghari, J. Ind. Eng. Chem. 20 (2014) 2421-2427.
[37] G. Absalan, A. Bananejad, M. Ghasemi, Anal. Bioanal. Chem. Res. 4 (2017) 65-77.
[38] F. Marahel, Iran. J. Chem. Chem. Eng. 38(5) (2019) 129-142.
[39] Sh. Bouroumand, F. Marahel, F. Khazali, Desal. Water Treat. 223 (2021) 388-392.
[40] H.S. Ghazimokri, H. Aghaie, M. Monajjemi, M.R. Gholami, Russian J. Phys. Chem. A. 96(2) (2022) 371-384.
[41] Sh. Davoudi, Iran. J. Chem. Chem. Eng. 42(1) (2023) 1-15. doi: 10.30492/IJCCE.2021.526904.4630.

مجله شیمی فیزیک و شیمی نظری
دانشگاه آزاد اسلامی واحد علوم و تحقیقات
جلد ۱۹، شماره ۲، تابستان ۱۴۰۱
ISSN ۱۷۳۵-۲۱۲۶

جذب اولتراسونیک بوتیل پارابن بر روی زئولیت ایمیدازولات-٦٧ سنتز اولتراسونیک اصلاح شده توسط نانوذرات اکسید آهن: یک روش طراحی تجربی (همراه باکاربرد پاسخ سطح)

محمد پورمحمد[۱]، آرزو قادی[۱*]، علی آقابابایی بنی[۲]

[۱] دانشگاه آزاد اسلامی واحد آمل، گروه مهندسی شیمی، واحد آیت الله آملی، دانشگاه آزاد اسلامی، آمل، ایران.
[۲] دانشگاه آزاد اسلامی واحد شهرکرد، گروه مهندسی شیمی، واحد شهرکرد، دانشگاه آزاد اسلامی، شهرکرد، ایران.

چکیده

کاربرد زئولیت ایمیدازولات-٦٧ اصلاح شده توسط نانوذرات اکسید آهن، برای حذف رنگ بوتیل پارابن از محلول های آبی مورد بررسی قرار گرفت. تکنیک‌های یکسانی از جمله BET، FT-IR، XRD، و SEM برای توصیف این ماده جدید استفاده شده‌اند. تأثیر متغیرهایی از جمله غلظت اولیه بوتیل پارابن (X1)، pH (X2)، دوز جاذب (X3)، و زمان فراصوت (X4) با استفاده از طراحی مرکب مرکزی (CCD) تحت روش سطح پاسخ (RSM) مورد بررسی قرار گرفت. علاوه بر این، تأثیر pH محلول، مقدار نانوذرات، غلظت رنگ بوتیل پارابن و زمان تماس مورد بررسی قرار گرفت. آزمایش‌ها با استفاده از روش سطح پاسخ طراحی شده‌اند. در این مقاله مقادیر ۱۰/۰ میلی گرم برگرم، ۰/۰۳ گرم، ۷/۰، ٤/۰ دقیقه به ترتیب به عنوان مقادیر ایده آل برای غلظت بوتیل پارابن، جرم جاذب، مقدار pH و زمان تماس در نظر گرفته شد. مطالعات سینتیک و ایزوترم مناسب بودن مدل های مرتبه دوم و لانگمویر را برای سینتیک و ایزوترم جذب بوتیل پارابن بر روی جاذب ثابت کرد. ثابت شد که جاذب برای بیش از یک بار قابل بازیافت است. از آنجایی که تقریباً ۹۹/۵ درصد از بوتیل پارابن با ظرفیت جذب ایده آل ۱۱۰/۰ میلی گرم برگرم برای بوتیل پارابن در کوتاه ترین زمان حذف شد، بنابراین نه تنها فرآیند جذب کوتاه مدت به عنوان یک مزیت در نظر گرفته شد، بلکه مزایای استفاده از زئولتیک ایمیدازولات-٦٧ اصلاح شده توسط نانوذرات اکسید آهن نیز در نظر گرفته شد. نانوذرات مانند قابل بازیافت، ایمن بودن و مقرون به صرفه بودن آن را به ماده ای امیدوارکننده و قدرتمند برای تصفیه فاضلاب تبدیل کرده است.

کلید واژه‌ها: بوتیل پارابن؛ جذب؛ زئولیت ایمیدازولات-٦٧؛ طراحی مرکب مرکزی (CCD)؛ روش سطح پاسخ (RSM)

[*] مسئول مکاتبات: arezoo.ghadi@gmail.com